Structure and Bonding in Magnesium Difluoride Clusters: The MgF 2 Molecule

ARTICLE *in* THE JOURNAL OF PHYSICAL CHEMISTRY A · APRIL 2001

Impact Factor: 2.69 · DOI: 10.1021/jp0041656

3 AUTHORS, INCLUDING:

Evelio Francisco
University of Oviedo
103 PUBLICATIONS **2,881** CITATIONS
SEE PROFILE

Aurora Costales
University of Oviedo
60 PUBLICATIONS **1,496** CITATIONS
SEE PROFILE

Structure and Bonding in Magnesium Difluoride Clusters: The MgF_2 Molecule

E. Francisco,* A. Costales, and A. Martín Pendás

Departamento de Química Física y Analítica, Facultad de Química, Universidad de Oviedo, E-33006 Oviedo, Spain

Received: November 10, 2000; In Final Form: February 2, 2001

We have calculated the ground-state geometry, vibrational frequencies, and bonding properties of MgF_2 at the Hartree−Fock (HF), second-order (MP2), and fourth-order Møller−Plesset (MP4(SDTQ)) levels of calculation. Several high-quality basis sets have been used, with special attention on the influence of polarization and diffuse functions on the above properties. The best HF and MP2 calculations predict that MgF_2 is a linear molecule. MP2 and MP4 results are very similar. The MP2 symmetric (ν_1) and asymmetric (ν_3) stretching frequencies are about 5−7% smaller than the HF values and agree well with the observed data. The MP2 ν_2 (bending) frequency is close to that found in other ab initio calculations and the experimental gas-phase value but is 80 cm^{-1} smaller than the value observed in the IR spectrum of MgF_2 trapped in solid argon. Polarization functions shorten noticeably the magnesium−fluorine equilibrium distance and increase ν_1 and ν_3. An atoms in molecules (AIM) analysis of the wave functions reveals that MgF_2 is a highly ionic molecule, the net charge of Mg being about +1.8 e, and that most basis set effects are due to the poor convergence properties of the atomic electron dipole moments. This suggests a polarizable ions model that is shown to account for the trends found in most of the properties studied. The origin of the bending problem in these compounds is traced back to the polarizability of the cation.

I. Introduction

Alkaline earth dihalide clusters $(AX_2)_n$ are known to exist both in the gas phase at high temperature and low pressure and trapped in solid matrixes. Monomers and dimers have been the subject of different experimental,[1−10] atomistic,[11−14] and theoretical studies.[15−28] The symmetry of ground-state isolated AX_2 molecules is known to vary from $D_{\infty h}$ to C_{2v} as the A and X atomic numbers increase. Most experiments on them, therefore, have tried to elucidate the stability of the linear versus the bent configurations and the influence of a matrix environment on their vibrational spectra.[6,7] Available experimental information on $(AX_2)_n$ ($n > 1$) arise mostly from the analysis of their Infrared (IR) and Raman spectra in solid matrixes.[4−7] Except at very low concentrations, the AX_2 molecules dimerize, or even trimerize, easily.[7] The formation of these polymeric species sometimes precludes a straightforward assignment of the vibrational bands of the monomer, dimers, and trimers, and quantum mechanical insights become necessary for a proper understanding of these species.

On the theoretical side, the influence of basis set effects on the monomers' molecular geometry has received special attention in recent years,[19−23] and some studies concerning the effects of the basis set on their molecular orbitals have also been published.[15,16] Atomistic methods have been used by Gigli[14] in $(AX_2)_2$ clusters and by Martin[13] in $(CaF_2)_n$ ($n = 1−6$) clusters. More recently, Eichkorn et al.[27] have performed SCF, second-order Møller−Plesset (MP2) and coupled-cluster calculations on $(MgCl_2)_n$ ($n = 1−24$) clusters and Molnár et al.[26] have investigated $(MgCl_2)_n$ ($n = 1−2$) clusters at the SCF and MP2 levels. Magnesium difluorides and dichlorides have also been studied by Axten et al.,[23] and beryllium and magnesium fluorides and chlorides, by Ystenes.[25]

In this and the following paper, referred to as papers I and II, respectively, we report the results of first-principles calculations on $(MgF_2)_n$ ($n = 1−3$) clusters. Our aim is to analyze quantitatively high-quality basis sets and correlation energy effects on the geometry, vibrational spectra, and bonding properties of these systems. Electron correlation has been included using standard Møller−Plesset perturbation theory. No density functional (DFT) approaches have been used, to avoid any dependence of the results on the choice of functionals. The simultaneous analysis of the monomer, dimers, and trimers will allow us to study how some of the above properties change with the cluster size and to what extent they are transferable on passing from the MgF_2 molecule to bigger clusters. In this respect, our focus will be centered on the evolution of group frequencies, bonding properties, and Mg−F distances for similarly coordinated Mg atoms with cluster size. The building up of clusters from small units, a more complex issue here than in alkali metal halides due to the 1:2 stoichiometry of the $(AX_2)_n$ systems, has also been investigated.

As the nature of the Mg−F interaction is concerned, and as far as we know, all studies of $(AX_2)_n$ clusters have been carried out in terms of standard molecular orbital theory, using Mulliken and/or Löwdin electron population analyses. This fact artificially centers the attention on orbital explanations to every question about molecular properties, leaving physical mechanisms behind. In view of the large ionic contributions to bonding that are to be expected in these compounds, we feel that a theoretically well-founded framework, like the theory of atoms in molecules[29] (AIM), might shed light on the origin of some of the poorly understood characteristics of these systems. In light of this theory, $(MgF_2)_n$ clusters will reveal themselves as largely ionic species at any level of study. The local analysis of the electron density and Laplacian scalar fields at particular critical points,

10.1021/jp0041656 CCC: $20.00
Published on Web 03/30/2001

TABLE 1: Definition of Basis Sets and Contraction Schemes Used in This Work

basis set[a]	Mg	contraction	F	contraction
6-31[b]	[4s/3p]	(6631/631)	[3s/2p]	(631/31)
6-311[c]	[6s/5p]	(631111/42111)	[4s/3p]	(6311/311)
TZV[d]	[6s/5p]	(631111/42111)	[5s/3p]	(62111/411)
TZV(1d)[e]	[6s/5p/1d]	(631111/42111/ 1)	[5s/3p/1d]	(62111/411/1)
TZV(2d1f)[f]	[6s/5p/2d/1f]	(631111/42111/ 2/1)	[5s/3p/2d/1f]	(62111/411/2/1)
TZV(3d1f)[g]	[6s/5p/3f/1f]	(631111/42111/ 3/1)	[5s/3p3d/1f]	(62111/411/3/1)
TZV(1d)+[h]	[7s/6p/1d]	(6311111/42111 1/1)	[6s/4p/1d]	(621111/4111/1)
TZV(3d1f)+[h]	[7s/6p/3d/1f]	(6311111/42111 1/3/1)	[6s/4p/3d/1f]	(621111/4111/3/ 1)

[a] Cartesian basis sets (i.e. 7 d-like and 10 f-like Gaussian functions) have been used in this work. [b] Basis set of Francl et al. for Mg[32] and basis set of Hehre et al. for F.[33] [c] Basis set of McLean and Chandler for Mg[34] and basis set of Krishnan et al. for F.[35] Note that, according to the standard notation, the label 6-311 is only correct for F, as the contraction scheme of Mg in this basis set is (631111/42111). [d] Similar to the 6-311 basis set for Mg and basis set of Dunning for F.[36] [e] Obtained by adding a d-type Gaussian primitive ($\alpha_d(Mg) = 0.234$, $\alpha_d(F) = 1.62$) to the Mg and F TZV basis set. [f] Obtained by adding two d-type ($\alpha_d(Mg) = 0.468$, $\alpha_d(Mg) = 0.117$, $\alpha_d(F) = 3.24$, $\alpha_d(F) = 0.81$) and one f-type ($\alpha_f(Mg) = 0.2$, $\alpha_f(F) = 1.85$) Gaussian primitives to the Mg and F TZV basis set. [g] Obtained by adding three d-type and one f-type Gaussian primitives to the Mg and F TZV basis set. The d exponents are defined as follows: if the two d exponents of the TZV(2d1f) basis set are ζ_1 and ζ_2 ($\zeta_2 < \zeta_1$), the three d exponents in the TZV(3d1f) basis are $2\zeta_1$, $2\zeta_2$, and $\zeta_2/2$. The f exponent are similar to that of the TZV(2d1f) basis. [h] TZV(1d)+ and TZV(3d1f)+ bases are obtained by adding a diffuse s-type and a diffuse p-type primitives with a common exponent ($\alpha_{sp}(Mg) = 0.0146$, $\alpha_{sp}(F) = 0.1076$) to the TZV(1d) and TZV(3d1f) bases, respectively.

together with the study of atomic electronic multipole moments, has allowed us to isolate the dependence of different physical observables on basis set and correlation effects. It turns out, for example, that atomic monopoles (atomic charges) are already saturated with small basis sets, while atomic dipoles (which are crucial to determine whether the linear or bent equilibrium geometries of the monomers are preferred and which depend on atomic polarizabilities) need extremely large polarized basis sets to achieve similar levels of saturation. This explains the theoretical difficulty to assess the ground-state geometry of borderline molecules such as CaF_2. The AIM analyses will allow us to recast the ab initio results into a very useful physical model of polarizable point ions with almost nominal charges and constant polarizabilities that interact by means of electrostatic forces and short-range repulsive potentials.

Paper I is devoted to the MgF_2 molecule. We have performed calculations with several good-quality basis sets and at different levels of theory to determine basis set and correlation effects on molecular and AIM properties. Though better studied than their polymeric species, MgF_2 still presents some uncertain aspects that are important on their own. It is unclear, for example, why the bending ν_2 frequency, predicted to be in the range $\simeq 155-165$ cm^{-1} in all previous calculations, differs so much from the measured value in a solid matrix ($\simeq$249 cm^{-1}). Since, except in the work of Ramondo et al.,[24] vibrational frequencies have been always obtained at the SCF level, it seems necessary to analyze whether correlation effects bring ν_2 into agreement with the observed data or the discrepancy is indeed a matrix effect. Moreover, correlation effects at the MP4 level and using basis sets of quality triple-ζ or higher on the structure, energetic properties, and bonding of MgF_2 are not known. In this way, it will turn clear which basis set and level of calculation are necessary to obtain results of enough and uniform quality for dimers and trimers, which will be considered in paper II.

The rest of the paper is organized as follows. In section II we will give some details on the calculations and will describe the basis sets used in our work. In section III, correlation and basis set effects on the geometry, energetic quantities, and harmonic vibrational frequencies will be discussed. A survey of the previously studied molecular properties and a discussion of the nature of the interactions in the light of the AIM theory are presented in section IV. In section V we will integrate all the previous data into a coherent explanation of the behavior of the MgF_2 molecule and will also introduce the polarizable ions model. Finally, in section VI we will summarize our conclusions.

II. Details of the Calculation

Restricted HF, MP2, and MP4 calculations have been done on the MgF_2 molecule in order to determine its equilibrium geometry in the singlet ground state. MP2 calculations have been performed with the GAMESS system of programs, using the usual frozen-core convention.[30] MP4 data, including single, double, triple, and quadruple excitations (SDTQ), were obtained with the GAUSSIAN 98 package.[31] HF, MP2, and MP4 bending (ν_2), symmetric stretching (ν_1), and asymmetric stretching (ν_3) harmonic frequencies have been computed at the corresponding HF, MP2, or MP4 optimized geometries. Default methods to compute the Hessian matrixes have been used both in GAMESS and in GAUSSIAN 98 calculations, i.e., analytic derivatives for HF and MP2 results and numerical ones for MP4 calculations. We have made extensive analyses of the convergence of properties with the quality of the basis sets. For the sake of brevity, we will only present and discuss here results obtained with the representative basis set ensemble defined in Table 1.

III. Structural and Energetic Properties

A. Geometry. Although there exists a general consensus about the linear geometry of MgF_2 in the gas phase and practically every quantum chemical simulation predicts a linear ground state, the difficulties posed by the CaF_2 case[20] more than justify a careful revision of the problem. We have therefore performed HF and MP2 optimizations of the Mg−F distance, R(Mg−F), at fixed bending angle, α, the latter decreasing from 180° (linear configuration) to 100°, and using the TZV and TZV(3d1f)+ basis sets. The evolution of the total molecular energy (referred to that of the linear configuration, ΔE) and the Mg−F distance versus α are displayed in Figures 1 and 2, respectively. MgF_2 is always predicted to be linear, no matter the calculation is a HF or MP2 one nor the basis set is TZV or TZV(3d1f)+. Moreover, an energetically higher bent isomer is not predicted. It is noticeable that the four curves in Figure 1 practically coincide; i.e., electron correlation effects do not bend the molecule and have a very limited effect on the ground-state potential energy surface in the nearness of its minimum. Our ΔE values are very similar to those reported in refs 15, 16, and 19. For instance, ΔE at $\alpha = 120°$ is about 22.5 mhartree in the four calculations. A recent work on monomeric CaF_2[20] concluded that a very large d basis on Ca is necessary to account for the nonlinearity of this molecule. DeKock et al. also suggested that d orbitals on Ca are responsible for the nonlinearity. The weak dependence of ΔE on the d orbitals in the

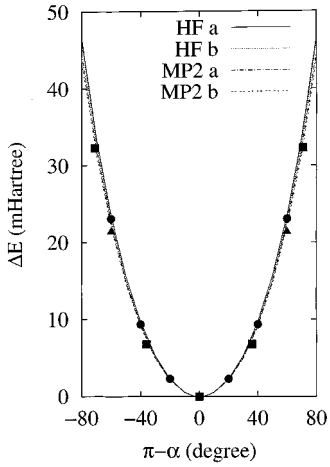

Figure 1. Bending energy of MgF_2, $\Delta E = E(\alpha) - E(180)$, using the TZV (a) and TZV(3d1f)+ (b) basis sets. The HF values given by Astier et al.,[15] Gole et al.,[16] and DeKock et al.[19] are indicated by squares, circles, and triangles, respectively.

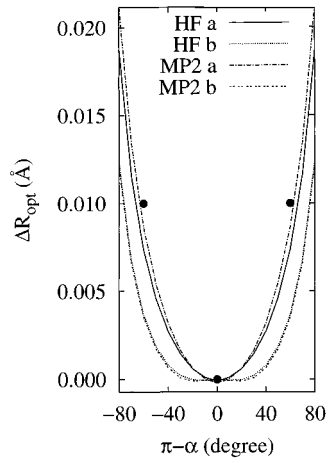

Figure 2. Change of the Mg−F equilibrium distance (R_{opt}) with respect to its value in the linear configuration as a function of the bending angle α. Letters a and b stand for the TZV and TZV(3d1f)+ basis sets, respectively. The HF value given by DeKock et al.[19] is indicated by a circle.

present case shows that a further increase of the number of d functions or the optimization of the d exponents would not modify essentially our results. The significance of these results will become apparent after our AIM analysis of the atomic electron multipoles of the MgF_2 molecule and will suggest a simple appealing model that accounts easily for this variability.

Our results show that the equilibrium Mg−F distance is fairly insensitive to α, with R_{opt} increasing by less than 0.025 Å in the HF and MP2 TZV calculations and by less than 0.015 Å in the HF and MP2 TZV(3d1f)+ calculations, when α decreases from 180 to 100°. Correlation effects on $\Delta R_{opt}(\alpha) = R_{opt}(\alpha) - R_{opt}(180)$ are negligible for the TZV(3d1f)+ basis set and very small for the TZV basis. This result is in agreement with those reported by Kaupp et al.[22] for the alkaline earth dihalides. It is worth mentioning that whereas $R_{opt}(\alpha)$ is nearly parabolic in the HF and MP2 TZV curves, the functional dependence of R_{opt} with α in the HF and MP2 TZV(3d1f)+ calculations seems to be slightly more complex. Finally, our value of ΔR for $\alpha = 120°$ is very similar to that given by DeKock et al.[19] Given the clear evidence for the linear geometry of MgF_2 in our best calculations, we will focus our attention on this geometry in the following.

TABLE 2: Basis Set and Correlation Effects on the (Linear) Computed Geometry of MgF_2 (in Å)

basis set	R_{opt}(HF)	R_{opt}(MP2)	R_{opt}(MP4)
6-31	1.752	1.777	1.779
6-311	1.758	1.783	1.785
TZV	1.762	1.798	1.801
TZV(1d)	1.743	1.771	1.772
TZV(2d1f)	1.728	1.757	1.758
TZV(3d1f)	1.729	1.761	1.763
TZV(1d)+	1.740	1.769	1.770
TZV(3d1f)+	1.729	1.762	
Astier et al.[15,a]	1.77		
Pendergast and Hayes[18,b]	1.77		
DeKock et al.[19,c]	1.75		
Seijo et al.[21,d]	1.758		
Kaupp et al.[22,e]	1.753		
Ramondo et al.[24,f]	1.723	1.744	
Axten et al.[23,g]		1.763	
exptl[37]	1.770[h]		

[a] HF results using (12s/9p) and (12s/5p) basis sets for Mg and F atoms, respectively, contracted to a valence double-ζ basis and improved by additional free functions on Mg (1d) and F (1s,1p). [b] HF results using (9s/5p)[5s/3p] and (12s/10p/4d)[4s/2p/1d] basis for F and Mg atoms, respectively. [c] HF Slater results using [2s/2p/1d] and (4s/4p/3d) STO valence basis for F and Mg atoms, respectively. [d] HF results using (61/411/1) and (61/4111/1) valence basis sets for Mg and F, respectively, plus the Cowan−Griffin relativistic ab initio model potential (AIMP) method[39] to represent the 1s and 2s electrons for Mg and the 1s electrons for F. [e] HF results using the basis set of McLean and Chandler[34] for Mg [augmented by a diffuse sp set[35] and one d function[40] and in addition a 5s5p valence-electron basis set (plus one d-polarization function and a quasi relativistic pseudopotential to represent the two core-1s electrons) for F. [f] HF and MP2 results using a 6-31G* split-valence basis set. [g] MP2(full) result using a 6-311+G(2d) basis set. [h] Gas-phase electron diffraction experiment.

Our computed equilibrium Mg−F distances (R_{opt}) are compared with experiment and with other theoretical results in Table 2. At the three levels of calculation, R_{opt} increases from the 6-31 to the TZV basis. The inclusion of a first d polarization function in the TZV basis set shortens R_{opt} by 0.019, 0.027, and 0.029 Å in the HF, MP2, and MP4 calculations, respectively. A second d-type function and an f-type function additionally shorten R_{opt} by 0.014 Å. TZV(2d1f) calculation of R_{opt} seems to be basis set converged, as the inclusion of a third d-type and diffuse s and p functions hardly changes the Mg−F distance. As it will seen below and in our second paper,[38] polarization functions decrease Mg−F distances and increase the harmonic vibrational frequencies of $(MgF_2)_n$ ($n = 1-3$). This evidences a clear role of polarization in the accurate description of the potential energy surface of these clusters. As regards correlation effects, our MP2 R_{opt} values are 0.025, 0.025, and 0.028−0.036 Å greater than the corresponding HF values found for the 6-31, 6-311, and TZV bases, respectively. MP4 corrections increase R_{opt} by less than 0.004 Å in all cases. A geometry optimization of the $(MgF_2)_n$ clusters at the MP4 level seems thus to be unnecessary. It is to be noticed that the role of polarization on the equilibrium Mg−F distance is contrary in sign and similar in magnitude to that of correlation. This explains the good results obtained at the HF level with unpolarized basis sets.

B. Energetic Properties. Total energies at a variety of computational levels are shown in Table 3. As expected, total and correlation energies decrease with increasing basis set size. The 6-311 basis set is noticeably better than the 6-31, and the TZV basis set is slightly better than the 6-311. Diffuse s and p functions decrease the HF total energies by about 3 mhartree on passing from the TZV(1d)/TZV(3d1f) to the (TZV(1d)+/TZV(3d1f)+) basis and hardly contribute to the correlation energy. Contrarily to this, the (first two) d- and f-polarization

TABLE 3: Total Energy (hartree) of MgF_2 ($D_{\infty h}$)

basis set	HF	MP2(RHF)[a]	MP2	E_{corr}(MP2)	MP4
6-31	−398.552 859	−398.820 248	−398.820 762	−0.268 412	−398.824 905
6-311	−398.639 371	−398.939 357	−398.939 853	−0.301 003	−398.944 496
TZV	−398.668 162	−398.981 050	−398.982 026	−0.314 873	−398.987 718
TZV(1d)	−398.695 917	−399.150 460	−399.151 099	−0.455 834	−399.161 898
TZV(2d1f)	−398.710 400	−399.269 434	−399.270 163	−0.560 524	−399.287 190
TZV(3d1f)	−398.711 957	−399.278 631	−399.279 488	−0.568 432	−399.297 213
TZV(1d)+	−398.698 960	−399.156 891	−399.157 571	−0.459 287	−399.169 338
TZV(3d1f)+	−398.712 239	−399.279 364	−399.280 281	−0.568 980	

[a] MP2 energy at the HF geometry.

TABLE 4: Ionization Potential (eV) of MgF_2

basis set	HF	MP2	MP4	Koopmans[a]
TZV	13.599	14.429	14.149	15.398
TZV(1d)	13.717	14.498	14.190	15.447
TZV(2d1f)	13.721	14.725	14.419	15.491
TZV(3d1f)	13.729	14.780		15.510
TZV(1d)+	13.724	14.568	14.267	15.515
TZV(3d1f)+	13.727	14.789		15.518
exptl	13.3 ± 0.3,[b] 13.6 ± 0.2[c]			

[a] The IP is obtained as minus the orbital energy of the highest occupied molecular orbital of MgF_2 ($1\pi_g$). [b] Reference 9. [c] Reference 41.

functions reduce the MP2 (MP4) total energy by +0.288 (+0.299) hartree in the calculations with the TZV bases. The MP4 calculations decrease the MP2 total energies by about 3−6 and 10−20 mhartree when nonpolarized and polarized bases are used, respectively. Finally, it is worth mentioning that optimizing the geometry on passing from the HF to the MP2 calculations lowers the total energy by less than 1 mhartree in all the cases.

A better insight of the influence that basis set and correlation effects have on energetic magnitudes is gained if other properties, experimentally accessible, are studied. We have chosen the ionization potential (IP) ($MgF_2 \rightarrow MgF_2^+ + e$), the atomization energy (AE) ($MgF_2 \rightarrow Mg(^1S) + 2F(^2P)$), and the dissociation energy (DE) ($MgF_2 \rightarrow Mg^{2+}(^1S) + 2F^-(^1S)$). To obtain the vertical IP, we have performed spin-unrestricted HF, MP2, and MP4 calculations in the ground state of MgF_2^+ at the optimized geometry of MgF_2. Our results with the TZV bases are collected in Table 4. We predict a HF/TZV value of 13.6 eV, which is in very good agreement with the experimental value reported in refs 9 (13.3 ± 0.3 eV) and 41 (13.6 ± 0.2 eV). Polarization (and diffuse) functions modify the IP by just 0.1 eV. As expected, their effect in this kind of vertical transition is very limited. Given that the absolute value of the correlation energy is greater in MgF_2 than in MgF_2^+, MP2 calculations worsen slightly the agreement with experiment, yielding IP's 0.3−1.1 eV higher than the HF values. The MP4 calculations partially correct the MP2 results, providing IP's 0.2−0.3 eV uniformly smaller than the MP2 numbers. Ignoring electron density reorganizations (a là Koopmans) in passing from MgF_2 to MgF_2^+ generates IP's about 7% higher than the experimental and the HF values obtained as differences between the total energies of MgF_2 and MgF_2^+.

The AE and DE values are collected in Table 5. The HF/6-31, HF/6-311, and HF/TZV calculations produce very similar AE values. The use of polarization functions increases the AE by 0.8−2.0 eV (10−30%), due to the better variational performance of the polarized basis sets in the molecule. Diffuse s and p functions change the AE by less than 0.1 eV (≃1%). Our HF AEs are 2−3 eV (20−30%) smaller than the experimental result[9,41] and the Hartree−Fock−Slater value reported by DeKock et al.[19] The HF/6-31 and HF/6-311 DE values are

TABLE 5: Atomization (AE) and Dissociation Energy (DE) (eV) of MgF_2

basis set[a]	AE(HF)	DE(HF)	DE(MP2)	DE(MP4)
6-31	6.494	28.320	28.926	
6-311	6.743	27.500	25.012	
TZV	6.874	26.117	23.107	21.866
TZV(1d)	7.629	26.872	27.708	26.605
TZV(2d1f)	8.023	27.266	30.947	30.014
TZV(3d1f)	8.066	27.308	31.201	30.287
TZV(1d)+	7.712	26.955	27.884	26.807
TZV(3d1f)+	8.073	27.316	31.223	
DeKock et al.[b]	10.539			
exptl	10.669,[c] 10.628[d]	26.759[e]		
rutile, exptl[f]		30.64		

[a] The total energies of Mg and F atoms and ions have been computed with the same basis sets used in the molecule but removing the polarization and diffuse functions. [b] Reference 19. [c] Reference 9. [d] Reference 41. [e] Reference 2. [f] Reference 42.

TABLE 6: Harmonic Vibrational Frequencies (ν_1, ν_2, ν_3) of MgF_2 (cm^{-1})

basis set	HF	MP2	MP4
6-31	(578, 130, 914)	(551, 119, 874)	(546, 118, 867)
6-311	(572, 135, 909)	(544, 124, 869)	(543, 122, 865)
TZV	(557, 155, 883)	(519, 148, 827)	(517, 146, 822)
TZV(1d)	(582, 163, 914)	(554, 156, 872)	(553, 155, 869)
TZV(2d1f)	(592, 155, 928)	(559, 140, 879)	(560, 135, 878)
TZV(3d1f)	(589, 157, 920)	(551, 151, 864)	
TZV(1d)+	(588, 166, 920)	(553, 157, 871)	(552, 155, 867)
TZV(3d1f)+	(588, 157, 918)	(549, 151, 859)	
ref 43	(630, 330, 990)		
ref 18c	(533, 295, 990)		
ref 14	(641, 156, 849)		
ref 21c	(579, 151, 927)		
ref 22c	(580, 155, 912)		
ref 24c	(614, 150, 962)	(587, 150, 920)	
exptl[37]	(540, 165, 825)[a]		
exptl[7]	(550, 249, 842)[b]		

[a] Gas-phase electron diffraction experiment. [b] Infrared/Raman spectra of MgF_2 trapped in solid argon. [c] See Table 3 for the definition of the basis set and type of calculation.

2−4 eV (5−14%) larger than the observed values,[2] whereas the HF/TZV calculations yield DE's in remarkable agreement with the experiment. As shown in Table 5, correlated MP2 DE values are slightly worse than HF results. It is interesting to remark that the addition of polarization functions change the sign of the MP2 corrections to the DE's. MP4 calculations decrease the MP2 values for DE by 1 eV (2−4%). Finally, it is worth to mention that AE's and DE's do not appreciably improve when the atomic (ionic) total energies are computed using the counterpoise method to correct for the basis set superposition error (BSSE).[44]

C. Vibrational Frequencies. The computed vibrational frequencies ν_1 (symmetric stretching), ν_2 (bending), and ν_3 (asymmetric stretching) of MgF_2 are collected in Table 6. MP2 calculations reduce ν_1 and ν_3 by about 5−7% with respect to

the HF values. MP2 ν_2 values are also smaller than the HF values, although the reduction is not easily related to the size of the basis set or to the inclusion of polarization (and diffuse) functions. MP4 frequencies are 0−7 cm^{-1} smaller than the MP2 results.

The inclusion of a first d polarization function raises the computed frequencies by roughly 3−7%. Adding a second d function and the f polarization function also increases ν_1 and ν_3. The bending frequency (ν_2), however, decreases from 163 (156) to 155 (140) cm^{-1} in passing from the HF(MP2)/TZV-(1d) to the HF(MP2)/TZV(2d1f) calculation. When the third d function is included, ν_1 and ν_3 decrease a few wavenumbers but, again, ν_2 shows an opposite tendency. Our exploration with other basis sets has evidenced the strong dependence of ν_2, not only on the number of d polarization functions but on the orbital exponents of these functions. The crucial role played by the d basis functions on determining ν_2 is obviously related to the discussion on the linearity of the alkaline earth molecules.[15,16,19,21,22] In contrast, the diffuse s and p functions have very little influence on the computed ν_1, ν_2, and ν_3 values. It is interesting to remark that ν_1 and ν_3 turn out to be very close to the experiment[7,37] in our best MP2 calculation (TZV(3d1f)+).

In all these arguments, it is important to isolate direct basis set and correlation effects from indirect contributions. As it can directly be seen from a comparison of Tables 2 and 6, a most important, probably outweighing factor controlling ν_1 and ν_3 is the Mg−F distance at which frequencies are computed. There is a very strong, intuitive correlation among the stretching frequencies and the bond distance that is independent of direct basis set or correlation effects and that superimposes on them. On the contrary, ν_2 is much less prone to this influence, revealing again the importance of polarization functions to account for the bending problem. A direct effect we have observed in our explorations is a noticeable tightening of the bending frequency as the variational freedom of a nonpolarized basis set is increased and the optimal Mg−F distance increases. This is followed by a frequency decrease on introducing polarization functions in the basis set coupled to a decrease in the bond distance. These odd influences will be rationalized below. Our results, as those reported by Ramondo et al.,[24] support the idea that ν_1 and ν_3 should decrease when correlation effects are properly considered. Moreover, since MP4 calculations hardly change the MP2 results, it is reasonable to conclude that correlation corrections at the MP2 level are accurate enough to compute ν_1 and ν_3.

Finally, and concerning the comparison of ν_2 with the experiment, some comments are necessary. Previous SCF calculations[14,21,22] predicted values for ν_2 close to 155 cm^{-1}, in agreement with our own HF result. Considering that direct correlation effects at the MP2 and MP4 levels decrease slightly the SCF ν_2 frequency, we conclude, in agreement with Kaupp et al.[22] (see also references quoted in this paper), that the 165 cm^{-1},[37] gas-phase ED value should be validated and that the 249 cm^{-1}[17] value observed for the molecule trapped in solid argon reflects a large environmental influence.

IV. Bonding in Light of the AIM Theory

According to the AIM theory, developed by Bader et al.,[29,45−49] the basic laws of quantum mechanics are fulfilled within a molecular subsystem if and only if it is surrounded by a zero-flux surface, i.e., a surface fulfilling $\nabla\rho(\vec{r})\cdot\vec{n} = 0$ at each point. In this equation $\rho(\vec{r})$ is the electron density scalar field of the system and $\vec{n}$ is the unit vector normal to the surface. Most subsystems house a single nucleus in their interior and are called atoms. Any quantum mechanical observable, like the kinetic energy or the number of electrons, may be objectively partitioned into atomic contributions. For example, the net charge of an atom is obtained by integration of ρ over its attraction basin. According to the AIM theory, the basic structural elements of a molecule are related to the critical points of ρ. In particular, a bond critical point (BCP) is a first-order saddle point of ρ. The value of ρ at a BCP is clearly related to the bond order and the bond strength. Moreover, several scalar functions of the electron density, like its Laplacian, $\nabla^2\rho$, or the electron localization functions (ELF), have been successfully related to the nature of the chemical bond. For instance, $\nabla^2\rho$ informs about the accumulation ($\nabla^2\rho < 0$) or depletion ($\nabla^2\rho > 0$) of ρ at a point with respect to its immediate neighborhood. Large, negative values of $\nabla^2\rho$ at the BCP's are prototypical of covalent systems, while small positive ones appear in ionic or van der Waals systems.

It is usually possible to extract relevant physical models of molecular behavior from AIM analyses. As we will show below, in largely ionic systems, like the MgF_2 molecule of this work, the emergent picture is that of Coulombic forces among almost nominal ionic charges modified by multipolar fields arising from the extended nature of the electron density. To this end it is useful to obtain the electron atomic multipoles for each quantum basin in the system. In our case, a semiclassical simulation of the dominant interactions will allow us to rationalize many of the findings previously presented concerning basis set and correlation effects in the properties of the MgF_2 molecule. These ideas will serve as guiding principles in the study of bigger clusters. We will review the properties of the electron density scalar fields at relevant points, followed by a study of the electron multipoles of the quantum subsystems.

Previous studies in a large number of molecules have demonstrated that basis set effects in density-related properties are considerably larger than those found for geometric or energetic properties.[51] For this reason, we only consider here the AIM results corresponding to the TZV bases. In Table 7, we present the values of the BCP, ρ(BCP), $\nabla^2\rho$(BCP), and net charges of Mg and F atoms at the HF, MP2, and MP4 levels of calculation.

Some conclusions about the AIM analysis are best obtained from Figure 3. As found when considering the harmonic vibrational frequencies, an important indirect effect accounts for most of the basis set and theoretical level variability of these properties. Different levels of calculation give different positions for the BCP, but such positions correlate linearly with the corresponding Mg−F distance R_{opt}. Furthermore, the functions ln ρ and $\nabla^2\rho$ evaluated at the BCP position are also linear when plotted versus the BCP coordinate. This is the behavior predicted by the tail model of valence densities, according to which the bonding densities can be approximated by the superposition of exponentially decaying functions centered at each bonded nucleus.[52] This means that the AIM properties of MgF_2 are fairly independent of the basis set used (provided this is a high-quality one) and the level of the calculation. The rather different values of ρ(BCP) and $\nabla^2\rho$(BCP) are mainly due to the changes in R_{opt}. Moreover, the ratios of cationic and anionic radii seem to be quite stable along the series of calculations considered in this work. This conclusion is stressed if we recall the topological properties of the electron density of solid MgF_2, recently reviewed.[53] From Table 7 it is seen that both the density and its Laplacian vary continuously on passing from the isolated molecule to the solid, if the different equilibrium distances are taken into account.

TABLE 7: Topological Atoms in Molecules (AIM) Properties of MgF_2. BCP position, ρ(BCP), and $\nabla^2\rho$(BCP) in Å, e/Å^3, and e/Å,^{5} Respectively

basis set	BCP[a]	r_+/r_-[b]	ρ(BCP)	$\nabla^2\rho$(BCP)	q(Mg)
			HF Results		
TZV	0.7943	0.8208	0.4886	17.755 898	1.814 ± 0.000
TZV(1d)	0.7837	0.8169	0.5399	19.533 977	1.826 ± 0.000
TZV(2d1f)	0.7719	0.8073	0.6107	20.803 765	1.814 ± 0.091
TZV(3d1f)	0.7751	0.8126	0.6074	20.040 533	
TZV(1d)+	0.7819	0.8161	0.5507	19.721 128	1.825 ± 0.000
			MP2 Results		
TZV	0.8094	0.8187	0.4447	15.038 425	1.766 ± 0.000
TZV(1d)	0.7960	0.8164	0.5007	17.091 760	1.786 ± 0.000
TZV(2d1f)	0.7861	0.8097	0.5561	17.973 293	1.795 ± 0.000
TZV(3d1f)	0.7909	0.8153	0.5466	17.120 100	1.796 ± 0.000
TZV(1d)+	0.7947	0.8157	0.5088	17.167 478	1.784 ± 0.000
TZV(3d1f)+	0.7912	0.8150	0.5453	17.051 105	1.795 ± 0.000
			MP2 at the HF Geometry		
TZV	0.7968	0.8255	0.4879	17.177 841	1.766 ± 0.000
TZV(1d)	0.7863	0.8219	0.5372	18.976 380	1.785 ± 0.001
TZV(2d1f)	0.7760	0.8151	0.5993	20.022 483	1.794 ± 0.001
TZV(3d1f)	0.7795	0.8210	0.5945	19.269 083	1.794 ± 0.002
TZV(1d)+	0.7846	0.8212	0.5480	19.144 493	1.784 ± 0.001
TZV(3d1f)+	0.7795	0.8210	0.5945	19.264 264	1.795 ± 0.000
			MP4 Results		
TZV	0.8102	0.8177	0.4407	14.925 956	1.768 ± 0.002
TZV(1d)	0.7960	0.8156	0.4994	17.092 507	1.789 ± 0.000
TZV(1d)+	0.7947	0.8148	0.5081	17.167 912	1.787 ± 0.000
rutile(a)[c]	0.8663	0.797	0.2672	9.461 1	1.889 ± 0.000
rutile(b)	0.8790	0.799	0.2369		

[a] Bond critical point z in the notation (0,0,z), where (0,0,0) and (0,0,R_{opt}) are the coordinates of Mg and F, respectively. [b] Ratio between the Mg and F topological radii. [c] From ref 53. In rutile there are two (a, b) slightly different Mg−F bonds.

The electronic charge monopoles, or atomic charges, have been largely used to describe bonding type along the years. It is also known that most methods used to obtain those charges, like Mulliken's population analysis, lack theoretical foundation. By contrast, the AIM charges, collected in Table 7, have been obtained for Mg and F by integration of the electron density over their corresponding atomic basins. This procedure has a sound theoretical origin, as explained in detail elsewhere.[29] The net charge of Mg (q_{Mg}) is close to +1.8 e, indicating that the Mg−F bond is highly heteropolar, in agreement with traditional thinking. The global effect of polarization and diffuse functions is to increase q_{Mg}, making MgF_2 slightly more ionic. This fact has usually been explained as an enhancing of the charge transfer as the variational flexibility of the basis is increased. On the contrary, inclusion of correlation effects decreases q_{Mg}. As the MP2 net charges computed at the HF and MP2 geometries are practically the same, we conclude that charge transfer does not change appreciably with R(Mg−F), at least for values close to R_{opt}. Moreover, we notice that the point-charges dissociation energy of MgF_2 (without taking into account the widely screened F−F repulsion) is computed as 32.54 eV using nominal charges, but it decreases to 26.36 eV (in excellent agreement with our top MP4 result) if topological charges are used instead. This result is in the usual 10% window of agreement between electrostatic and actual lattice energies in highly ionic crystals such as NaCl. It is also interesting to observe how the Mg net charge in the solid (+1.89) is slightly larger than in the monomer, a result that is also in agreement with traditional reasoning. The overall energetics of the system is then very well explained by a simple ionic model.

Other evidence of the high ionicity of MgF_2 is given by $\nabla^2\rho$(BCP). Its value in the bonding region is large and positive. Figure 3d shows $\nabla^2\rho$ (HF/TZV(1d)+) in a plane containing the Mg and the two F atoms. Once again, it is clearly seen that the Mg−F bonds are prototypical closed-shell interactions: The Mg atom has completely lost its outermost electron shell (the 3s electrons of neutral Mg), giving almost a complete electron to each of the F atoms. It is also worth to mention the sphericity of the Mg electron pairs, whereas each of the F atoms has lost the spherical symmetry, yielding a net charge polarization in the binding region. Our solid-state results[53] reveal that this charge polarization has largely disappeared in the solid. Moreover, a deeper analysis of the interatomic surfaces separating the Mg and F atoms shows a very convex surface from the point of view of Mg and, thus, a very concave one for F. We have already shown[54] that convex and concave interatomic surfaces are characteristic of cationic and anionic roles, respectively.

Dipolar and quadrupolar electronic moments integrated over the atomic basins are shown in Table 8. The fluoride's dipole moment, at any theoretical level and using any basis set, shows a net displacement of the valence density toward the magnesium ion, in agreement with the behavior of the Laplacian just explored. This is the characteristic, well-known valence polarization of ionic compounds. A similar counterpolarization of the cation is not found here due to the cationic site symmetry. Both ions show densities compressed along the molecular axis, as evidenced by their appreciable positive quadrupole moments. Contrarily to the easy convergence of net charges with basis set and the overall small effect of correlation on its magnitude, the anion's dipole shows a very large dependence on the number and type of polarization functions in the basis set and a much smaller one on the presence of diffuse functions. To exclude interatomic distance effects, Table 8 also includes results from calculations with varying basis sets at the experimental MgF_2 geometry. From the joint analysis of both data sets it turns clear that the bond distance influence on the dipole is not large and that correlation effects are quite small and tend to increase the charge displacement. The presence of a large number of polarization functions is actually needed to allow for the non-

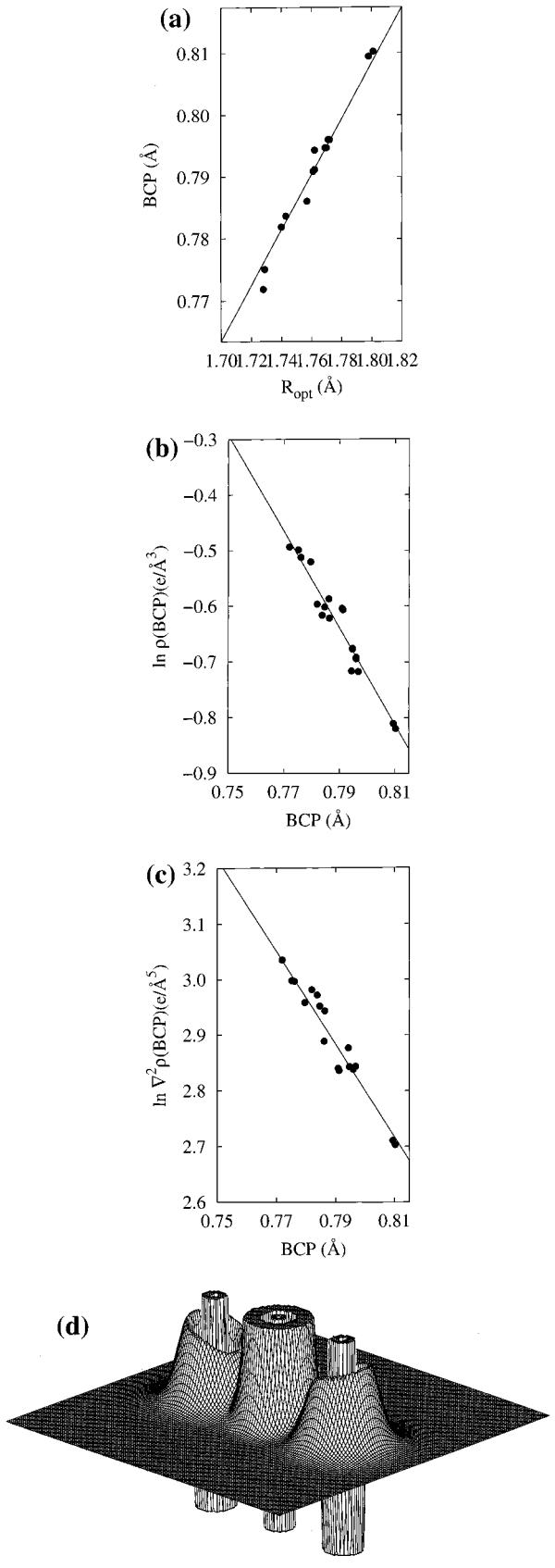

Figure 3. (a) Bond critical point position (BCP) versus R_{opt} according to the values collected in Tables 7 and 2, respectively. (b) Natural logarithm of the electron density at the BCP versus the BCP. (c) Natural logarithm of the Laplacian of the electron density at the BCP versus the BCP. (d) Laplacian of the electron density of MgF_2 at the HF geometry using the TZV(1d)+ basis in a plane containing the three atoms.

negligible valence polarization of the anions. The largest effect is found when including the first f-type function, as electronic displacements along the internuclear charges are best accounted for with odd parity functions. Atomic quadrupolar moments, in turn, show a better basis set convergence and do not seem to depend drastically on polarization functions. Correlation effects are also small and oscillatory at the MP2 and MP4 levels, the final effect being a slight increase in magnitude over HF values at fixed geometry. Q_{zz}, the molecular axis directed component of the traceless quadrupolar tensor, is positive for both ions, indicating oblate or compressed atomic electron densities. The anions turn out to be rather more bulky and compressed than the cation, such as bond point positions also point out.

We have also found interesting to make a comparison of the atomic properties of the MgF_2 atomic basins with those of other related compounds. For the sake of brevity we will only present a brief summary of the results on the fluoride's basin. We have made calculations in the NaF, F_2, and BeF_2 molecules at the HF/MP2/MP4 levels with the TZV basis sets of this section. In NaF, the fluoride's net charge is larger than in MgF_2, around -0.91 e. Its dipole moment also shows a valence polarization toward the cation that is again largely dependent on the number and type of polarization functions. Our best results stabilize about $\mu_z = 0.14$ au, which is around half the value obtained for the MgF_2 molecule, and point toward a constant ionic polarizability, as will be detailed below. The slightly larger value of Q_{zz}, around 1.23 au, is easily explained if the larger ionic size (bonded radius $r_b = 1.96$ au) is taken into account. Results on F_2 show that the substitution of the neighboring cation by a neutral species changes the sign of the polarization of the electron cloud of the fluorine atom. Even in this case, the back polarization of the fluoride, $\mu_z = 0.18$ au at the MP2/TZV-(3d1f) level, is very difficult to converge and depends strongly on polarization functions. Q_{zz}, on the contrary, easily stabilizes around 1.85 au at the MP2 level, showing a rather compressed neutral atomic basin. Calculations on the linear configuration of BeF_2 give a forward polarized fluoride with properties very similar to those of fluorides in MgF_2: $r_b = 1.67$ bohr, $q(F) = -0.889$ e, $\mu_z = 0.52$ au, and Q_{zz} 0.34 au in a MP2/TZV(3d1f)+ calculation. All these facts are consistent with the importance of the electron cloud polarization to account properly for the properties of ions even in largely ionic compounds.

V. Discussion and Modeling

The AIM analysis of the MgF_2 wave functions obtained in this work gives us a very detailed image of the prevalent interactions in this molecule. In the first place, the absence of the valence shell of the magnesium ion in the Laplacian field is a most clear sign of ionic behavior. Net ionic charges are very close to nominal, so the dissociation energy is well described by Coulombic terms. Neither integrated charges nor calculated dissociation energies are very sensitive to basis set or correlation effects, once geometrical changes on optimal geometries are taken into account.

Electron dipole moments, as stressed before, are much more difficult to converge, and the change of optimal geometries with basis set correlates cleanly with their magnitude. The effect is somewhat complex. The fluoride's dipole decreases as the size of a nonpolarized basis set increases: $\mu_z = 0.24$, 0.11, and 0.06 au for the STO-3G, 6-31, and TZV basis sets, respectively. This is coupled to a constant increase of Q_{zz}, which changes from 0.10 to 0.81 au. Very small, rigid basis sets do not show enough radial flexibility to face the nonspherical electric field felt by the anion and couple valence polarization to core polarization.

TABLE 8: Atomic Electron Dipoles, μ_z, and *zz* Components of Quadrupoles, Q_{zz}, in Linear Configurations of MgF_2[a]

basis set	$\lvert\mu_z\rvert$(F)	Q_{zz}(F)	Q_{zz}(Mg)	$\lvert\mu_z^e\rvert$(F)	Q_{zz}^e(F)
			HF Results		
TZV	0.0665	0.8070	0.3995	0.0709	0.7919
TZV(1d)	0.2403	0.7023	0.2722	0.2531	0.6467
TZV(2d1f)	0.3344	0.6062	0.3348	0.3114	0.6756
TZV(3d1f)				0.3192	0.7388
TZV(1d)+	0.2403	0.7424	0.2750	0.2532	0.6809
TZV(3d1f)+	0.2941	0.8170	0.2310	0.3152	0.7385
			MP2 Results		
TZV	0.1149	0.9283	0.5776	0.0972	0.9805
TZV(1d)	0.2934	0.7812	0.3915	0.2929	0.7831
TZV(2d1f)	0.3455	0.8872	0.3219	0.3531	0.8614
TZV(3d1f)	0.3456	0.9642	0.2988	0.3514	0.9467
TZV(1d)+	0.2848	0.8615	0.3874	0.2855	0.8586
TZV(3d1f)+	0.2848	0.8615	0.3874	0.2416	0.9421
			MP4 Results		
TZV	0.1152	0.9111	0.5808	0.0957	0.9682
TZV(1d)	0.2909	0.7626	0.3929	0.2899	0.7667
TZV(1d)+	0.2834	0.8381	0.3881	0.2834	0.8381

[a] Dipoles are directed from the magnesium toward the fluorides. The Mg−F distance is the experimental one in columns with the e superindex and the optimal for each basis set and theoretical level for the others. All data are in atomic units.

TABLE 9: Atomic Electron Multipoles versus Bending Angle, $\alpha = 180° - \beta$ at Selected β Values[a]

β (deg)	Q(F)	μ_y(F)	μ_z(F)	Q_{yy}(F)	Q_{zz}(F)	μ_z(Mg)	Q_{yy}(Mg)	Q_{zz}(Mg)
0	−0.8977	0.3372	0.0000	0.9558	−0.4778	0.0000	0.2925	−0.1462
1	−0.8976	0.3369	−0.0048	0.9552	−0.4779	−0.0005	0.2965	−0.1454
2	−0.8976	0.3368	−0.0096	0.9554	−0.4778	−0.0010	0.2966	−0.1455
5	−0.8976	0.3361	−0.0240	0.9551	−0.4773	−0.0024	0.2963	−0.1454
10	−0.8975	0.3342	−0.0477	0.9553	−0.4770	−0.0049	0.2951	−0.1455
20	−0.8974	0.3233	−0.0941	0.9569	−0.4754	−0.0105	0.2894	−0.1456
40	−0.8970	0.2835	−0.1832	0.9788	−0.4790	−0.0240	0.2579	−0.1503
80	−0.8954	0.1037	−0.3514	1.1506	−0.5430	−0.0543	0.1344	−0.1723

[a] The method and basis set employed is fixed to MP2/TZV(3d1f)+, and the Mg−F distance at each angle has been taken from Figure 2. The molecule is contained in the $y-z$ plane. All values except the angle β are in atomic units, and all sign conventions are as in the text. Notice the change of orientation at $\beta = 0$ with respect to previous data.

As a result, the density as a whole distorts toward the magnesium ion, and a large dipole emerges. Antiparallel dipoles on the fluorides have two opposite energetic effects: a large attractive charge−dipole interaction with the magnesium's net charge and a smaller repulsive dipole−dipole interaction. It is easy to show that the first effect outweighs the second. An electronic dipole on the fluorides, therefore, tends to decrease the Mg−F distance. This is exactly the effect found, R_{opt} shifting from 1.66 bohr to 1.76 bohr on going from the STO-3G to the TZV basis set. The inclusion of polarization functions into the basis set introduces angular variational flexibility, giving rise to a steady increase of the fluoride's dipole moment, as commented before. R_{opt} decreases accordingly. It is also easy to show that optimal geometries from different basis sets correlate rather well with their final dipoles. Finally, electron correlation displays its usual effects on geometries, both at the MP2 and the MP4 levels. The complex relationship between basis set and optimal geometry is then rationalized.

If we recall the clean correlation among the ν_1, ν_3 harmonic frequencies and the Mg−F distance, the conclusions of the last paragraph trace this effect back to polarization functions and a proper valence polarization of the electron density. As regards the bending problem, it is completely necessary to account also for the cation's polarization. To do that, we have integrated electron charges, dipoles, and quadrupoles over the ionic basins at each of the R(Mg−F)−α points of section IIIA. For the sake of brevity, Table 9 does only show results at the MP2/TZV-(3d1f)+ level at selected α values. It is easy to verify that both the fluoride and magnesium dipoles are proportional to the classical electric field felt by their nuclei at low β angles. We can calculate, then, effective atomic polarizabilities to predict atomic dipoles from nuclear electric fields. Using nominal charges at the MP2 level, these polarizabilities are about 2.2 au for the fluoride ion and about 0.62 au for the magnesium ion. If topological charges are used instead, the values increase to 2.3−2.4 and 0.69−0.73 au, respectively. These values should not be compared to solid-state polarizabilities, which include local electric field effects. Nevertheless, they are in agreement with chemical intuition. It is rather remarkable that the anion's polarizability, ξ_a, obtained under similar circumstances in our NaF calculations is about 2.3 au using nominal charges and 2.4−2.6 au using topological ones. These facts indicate a rather good transferability of dipole moments, pointing toward a simple model of polarizable ions with constant polarizability. The small but non-negligible polarizability of the magnesium, ξ_c, introduces a rich discussion that we will summarize now.

The role of ionic polarization on the molecular geometry can be understood by studying a model molecule in which the main sources of interatomic interactions are considered. As a result of the AIM analysis, such a model is that of point polarizable ions and, for example, simple power repulsive short-range potentials. By variation of the ionic polarizabilities, it is found that polarization has a 2-fold geometrical effect. On one hand, increasing polarizabilities decrease the interionic distance. This effect has already been commented, and it is only dependent on ξ_a as far as the linear geometry is preserved. If ξ_c is set to zero, the molecule collapses for all ξ_a values exceeding a limit, ξ_a^{lim}. This is the well-known polarization catastrophe, whose origin is to be traced to the independence of ξ's with geometry. All optimal geometries at $\xi_c = 0$ are linear. On the other hand,

TABLE 10: Results from Simulations on the MgF_2 Molecule within the Polarizable Ions Model[a]

ξ_c, ξ_a (au)	q(F) (e)	R(Mg−F) (Å)	(ν1, ν2, ν3) (cm^{-1})	μ_z(F) (au)
0.0, 0.0	1.00	1.652	(662, 174, 1037)	0.000
	0.90	1.712	(581, 148, 904)	0.000
	0.85	1.747	(542, 135, 843)	0.000
0.7, 2.3	1.00	1.579	(722, 172, 1038)	0.445
	0.90	1.650	(639, 147, 927)	0.350
	0.85	1.690	(584, 136, 866)	0.316

[a] See text for details.

a $\xi_a = 0$, $\xi_c \neq 0$ situation does not change R(Mg−F) in linear geometries. This is what one finds until a limit ξ_c value is reached, ξ_c^{bend}, at which the optimal geometry suddenly changes to nonlinear leaving a saddle at the linear configuration. Finally, if both polarizabilities are allowed to be nonzero, the ξ_c^{bend} value decreases with increasing ξ_a, approaching zero as ξ_a tends to ξ_a^{lim}. A continuous curve sets in, therefore, in a ξ_a, ξ_c map that completely separates linear from bent optimal geometries. It is absolutely necessary for the molecule to bend that the cation's polarizability be nonzero, the ξ_a value playing a secondary role by enhancing the tendency to bending at fixed ξ_c and by decreasing the final equilibrium angle α.

In the case under study, ξ_c is not large enough to bend the molecule but clearly influences the bending frequency, ν_2. To investigate this relation more deeply, we have made a simulation of the molecule under the model just presented. We have obtained realistic short-range pair potentials for the Mg−F and F−F couples according to the method described in ref 55. These have been used to optimize the molecular geometry and obtain the harmonic vibrational frequencies at equilibrium as a function of the ionic charges and the ionic polarizabilities. The main qualitative conclusion of this analysis is that ν_2 decreases with increasing optimal R(Mg−F), as expected but with a clear influence of ξ_c: the larger the polarizability the smaller the frequency. As R(Mg−F) in linear configurations is controlled basically by ξ_a, the interplay between both ionic polarizabilities, ultimately determined by the variational flexibility of the basis set, gives rise to the more complex behavior shown by ν_2 in Table 6. A summary of the simulation results with ionic polarizabilities taken from our AIM analysis and typical ionic charges is shown in Table 10. We see that ionic charges close to our topological values give equilibrium distances, harmonic frequencies, and anionic dipolar moments in rather good agreement with our top ab initio results.

The physical model emerging from these considerations is simple and in agreement with intuition. It also rationalizes the trends in the experimental geometries shown by the alkaline-earth dihalide triatomics and explains the reasons behind the theoretical difficulties in predicting these geometries. An AIM analysis of the AX_2 family in the light of the polarizable ions model is on demand and will be presented elsewhere.

VI. Conclusions

The equilibrium geometry and vibrational frequencies of MgF_2 have been investigated at the HF, MP2, and MP4 levels of calculation with 14 different high-quality basis sets. According to our results, R_{opt}(MP2) is 0.03−0.04 Å greater than R_{opt}(HF) and in good agreement with the experiment. In all the cases, MP4 correlation corrections modify R_{opt} by less than 0.004 Å with respect to the MP2 results. The inclusion of d and f functions in the basis set uniformly decreases R_{opt}, the reduction being larger for better basis sets. The effect of diffuse s and p functions on R_{opt} is negligible.

The exploration of basis set and correlation effects of the linear/bent structure of MgF_2 predicts undoubtedly that this molecule is linear in the gas phase. When the molecule is separated from the linear configuration, the total energy increases by the same quantity in both HF and MP2 calculations, independently of the inclusion of d polarization functions in the basis set.

At the MP2 level, the stretching frequencies ν_1 and ν_3 are predicted 5−7% smaller than their HF values and in good agreement with the experiment. These frequencies increase by 20−40 cm^{-1} when d and f polarization functions are used in the calculation. Contrarily to ν_1 and ν_3, the computed MP2 bending frequency, ν_2, is considerably smaller than the infrared/Raman observed value in solid argon. We agree with Kaupp et al.[22] that the matrix environment may have a strong influence on ν_2. We also conclude that ν_2 is strongly dependent on the halide basis set. As when geometry is considered, diffuse s and p functions have very little effect on the computed vibrational frequencies.

An AIM analysis of the obtained wave functions show that MgF_2 is a highly ionic molecule. The net charge of Mg is predicted to be q(Mg)$\simeq$ +1.82 e and q(Mg)$\simeq$ +1.80 e in the HF and MP2 calculations, respectively. Differences in ionicities on passing to the solid are not significant, and basis set and correlation effects do not modify the HF basin charges. Atomic electron dipole moments are the main responsible for the strong basis set effects found on the geometry and the harmonic frequencies of the MgF_2 molecule. These effects arise from the valence polarization suffered by the fluorides and the core polarization of the magnesium that accompanies bending. Dipoles converge very slowly and only after a large number of polarization functions have been included in the basis set, and their final values are found to be proportional to the classical electric fields felt by the basin nuclei. This gives rise to an appealing physical model of polarizable ions held together by electrostatic forces and short-range repulsions. This model explains beautifully most of the basis set effects on the calculated properties and is key to understand why other AX_2 systems are bent.

As a last important conclusion, we mention that MP2 and MP4 results are very similar, except in the case of the dissociation energy (2−3 eV greater in the MP4 than in the MP2 calculation). This result suggests that other AX_2 molecules can be safely investigated at the MP2 level.

Acknowledgment. We want to express our gratitude to Professors J. M. Recio and L. Pueyo for clarifying suggestions and the careful reading of the manuscript. Financial support from the Spanish Dirección General de Investigación Científica y Técnica (DGICYT), Project No. BQU2000-0466, is also acknowledged. We are also very grateful to R. W. F. Bader for providing our group with a copy of the AIMPAC suite of programs and to Mike Schmidt for promptly sending us the GAMESS program.

References and Notes

(1) Wharton, L.; Berg, R. A.; Kemperer, W. *J. Chem. Phys.* **1963**, *39*, 2023.

(2) Brewer, L.; Somayajulu, G. R.; Brackett, E. *Chem. Rev.* **1963**, *63*, 111.

(3) Büchler, A.; Stauffer, J. L.; Klemperer, W. *J. Am. Chem. Soc.* **1964**, *86*, 4544.

(4) Snelson, A. *J. Phys. Chem.* **1966**, *73*, 3028.

(5) Mann, D. E.; Calder, G. V.; Seshadri, K. S.; White, D.; Linevsky, M. J. *J. Chem. Phys.* **1967**, *46*, 1138. Calder, V.; Mann, D. E.; Seshadri, K. S.; Allavena, M.; White, D. *J. Chem. Phys.* **1969**, *51*, 2093.

(6) Hauge, R. H.; Margrave, J. L.; Kana'an, A. S. *J. Chem. Soc., Faraday Trans. 2* **1975**, *71*, 1082.
(7) Lesiecki, M. L.; Nibler, J. W. *J. Chem. Phys.* **1976**, *64*, 871.
(8) Beattie, I. R.; Jones, P. J.; Young, N. A. *Inorg. Chem.* **1991**, *30*, 2251; *J. Chem. Soc., Faraday Trans. 2* **1975**, *71*, 1082.
(9) Hildenbrand, D. L. *J. Chem. Phys.* **1967**, *48*, 3657.
(10) White, D.; Calder, G. V.; Hemple, S.; Mann, D. E. *J. Chem. Phys.* **1973**, *59*, 6645.
(11) Kim, Y. S.; Gordon, R. G. *J. Chem. Phys.* **1973**, *60*, 4332.
(12) Guido, M.; Gigli, G. *J. Chem. Phys.* **1977**, *66*, 3920.
(13) Martin, T. P. *J. Chem. Phys.* **1978**, *69*, 2036.
(14) Gigli, G. *J. Chem. Phys.* **1990**, *93*, 5224.
(15) Astier, M.; Berthier, G.; Millie, P. *J. Chem. Phys.* **1972**, *57*, 5008.
(16) Gole, J. L.; Siu, A. K. Q.; Hayes, E. F. *J. Chem. Phys.* **1973**, *58*, 857.
(17) Hayes, E. F.; Siu, A. K. Q.; Kisler, D. W. *J. Chem. Phys.* **1973**, *59*, 4587.
(18) Pendergast, P.; Hayes, E. F. *J. Chem. Phys.* **1977**, *68*, 4022.
(19) DeKock, R. L.; Peterson, M. A.; Timmer, L. K.; Baerends, E. J.; Vernooijs, P. *Polyhedron* **1990**, *9*, 1919.
(20) Hassett, D. M.; Marsden, C. J. *J. Chem. Soc., Chem. Commun.* **1990**, 667.
(21) Seijo, L.; Barandiarán, Z.; Huzinaga, S. *J. Chem. Phys.* **1991**, *94*, 3762.
(22) Kaupp, M.; Schleyer, P. v. R.; Stoll, H.; Preuss, H. *J. Am. Chem. Soc.* **1991**, *113*, 6012.
(23) Axten, J.; Trachtman, M.; Bock, C. W. *J. Phys. Chem.* **1994**, *98*, 7823.
(24) Ramondo, F.; Bencivenni, L.; Spoliti, M. *J. Mol. Struct. (THEOCHEM)* **1992**, *277*, 171.
(25) Ystenes, M.; Westberg, N. *Spectrochim. Acta, Part A* **1995**, *51*, 1501. Ystenes, B. K. *Spectrochim. Acta, Part A* **1998**, *54*, 855.
(26) Molnár, J.; Marsden, C. J.; Hargittai, M. *J. Phys. Chem.* **1995**, *99*, 9062.
(27) Eichkorn, K.; Scheneider, U.; Ahlrichs, R. *J. Chem. Phys.* **1995**, *102*, 7557.
(28) Lee, E. P. F.; Wright, T. G. *J. Phys. Chem.* **2000**, *104*, 974.
(29) Bader, R. F. W. *Atoms in Molecules*, 1st ed.; Oxford University Press: Oxford, U.K., 1990.
(30) Schmidt, M. W.; Baldridge, K. K.; Boatz, J. A.; Elbert, S. T.; Gordon, M. S.; Jensen, J. H.; Koseki, S.; Matsunaga, N.; Nguyen, K. A.; Su, S. J.; Windus, T. L.; Dupuis, M.; Montgomery, J. A. *J. Comput. Chem.* **1993**, *14*, 1347.
(31) Frisch, M. J.; Trucks, G. W.; Schlegel, H. B.; Scuseria, G. E.; Robb, M. A.; Cheeseman, J. R.; Zakrzewski, V. G.; Montgomery, J. A.; Stratmann, R. E.; Burant, J. C.; Dapprich, S.; Millam, J. M.; Daniels, A. D.; Kudin, K. N.; Strain, M. C.; Farkas, O.; Tomasi, J.; Barone, V.; Cossi, M.; Cammi, R.; Mennucci, B.; Pomelli, C.; Adamo, C.; Clifford, S.; Ochterski, J.; Petersson, G. A.; Ayala, P. Y.; Cui, Q.; Morokuma, K.; Malick, D. K.; Rabuck, A. D.; Raghavachari, K.; Foresman, J. B.; Cioslowski, J.; Ortiz, J. V.; Stefanov, B. B.; Liu, G.; Liashenko, A.; Piskorz, P.; Komaromi, I.; Gomperts, R.; Martin, R. L.; Fox, D. J.; Keith, T.; Al-Laham, M. A.; Peng, C. Y.; Nanayakkara, A.; Gonzalez, C.; Challacombe, M.; Gill, P. M. W.; Johnson, B. G.; Chen, W.; Wong, M. W.; Andres, J. L.; Head-Gordon, M.; Replogle, E. S.; Pople, J. A. *Gaussian 98 (Revision A.8)*; Gaussian, Inc.: Pittsburgh, PA, 1998.
(32) Francl, M. M.; Pietro, W. J.; Hehre, W. J.; Binkley, J. S.; Gordon, M. S.; DeFrees, D. J.; Pople, J. A. *J. Chem. Phys.* **1982**, *77*, 3654.
(33) Hehre, W. J.; Ditchfield, R.; Pople, J. A. *J. Chem. Phys.* **1972**, *56*, 2257.
(34) McLean, A. D.; Chandler, G. S. *J. Chem. Phys.* **1980**, *72*, 5639.
(35) Krishnan, R.; Binkley, J. S.; Seeger, R.; Pople, J. A. *J. Chem. Phys.* **1980**, *72*, 650.
(36) Dunning, T. H. *J. Chem. Phys.* **1971**, *55*, 716.
(37) Kasparov, V. V.; Ezhov, Y. S.; Rambidi, N. G. *J. Struct. Chem. (Engl. Transl.)* **1979**, *20*, 217; **1979**, *20*, 285; **1980**, *21*, 154.
(38) Francisco, E.; et al. To be published.
(39) Huzinaga, S.; Seijo, L.; Barandiarán, Z.; Klobu-kowski, M. *J. Chem. Phys.* **1987**, *86*, 2132. Seijo, L.; Barandiarán, Z.; Huzinaga, S. *J. Chem. Phys.* **1989**, *91*, 7011. Barandiarán, Z.; Seijo, L.; Huzinaga, S. *J. Chem. Phys.* **1990**, *93*, 5843.
(40) Andzelm, J.; Klobukowski, M.; Radzio-Andzelm, E.; Sakai, Y.; Tatewaki, H. *Gaussian Basis Sets for Molecular Calculations*; Huzinaga, S.; Elsevier: Amsterdam, 1984.
(41) *JANAF Thermochemical Tables*, 3rd ed.; Chase, M. W., et al., Eds.; The Dow Chemical Co.: Midland, MI, 1985.
(42) Baru, W. H. *Acta Crystallogr.* **1976**, *32*, 2200.
(43) Kim, Y. S.; Gordon, R. G. *J. Chem. Phys.* **1974**, *60*, 4332.
(44) Boys, S. F.; Bernardi, F. *Mol. Phys.* **1970**, *19*, 553.
(45) Bader, R. F. W. *Acc. Chem. Res.* **1975**, *8*, 34.
(46) Bader, R. F. W.; Srebrenik, S.; Nguyen-Dang, T. T. *J. Chem. Phys.* **1978**, *68*, 3680.
(47) Bader, R. F. W.; Nguyen-Dang, T. T. *Adv. Quantum Chem.* **1981**, *14*, 3663.
(48) Bader R. F. W.; Popelier P. L. A.; Keith T. A. *Angew. Chem., Int. Ed. Engl.* **1994**, *33*, 620.
(49) Bader, R. F. W. *Phys. Rev.* **1994**, *B49*, 13348.
(50) Allen, L. C. *J. Am. Chem. Soc.* **1989**, *111*, 9115.
(51) Mori, P. Private communication, 1998.
(52) Martín Pendás, A.; Costales, A.; Luaña, V. *J. Phys. Chem.* **1998**, *102*, 6937.
(53) Francisco, E.; Recio, J. M.; Blanco, M. A.; Martín Pendás, A.; Costales, A. *J. Phys. Chem.* **1998**, *102*, 1595.
(54) Luaña, V.; Costales, A.; Martín Pendás, A. *Phys. Rev.* **1997**, *B55*, 4285.
(55) Francisco, E.; Recio, J. M.; Blanco, M. A.; Martín Pendás, A. *Phys. Rev.* **1995**, *B51*, 2703.